

THE MESA HIGH POWER 1.3 GHz CW SOLID STATE POWER AMPLIFIER SYSTEMS*

R. Heine, F. Fichtner, C. Lorey

Institut für Kernphysik, Johannes Gutenberg-Universität Mainz, Mainz, Germany

Abstract

The Mainz Energy recovering Superconducting Accelerator MESA is a multi-turn energy recovery linac with beam energies in the 100 MeV regime currently under construction at Institut für Kernphysik (KPH) of Johannes Gutenberg-Universität Mainz. The main accelerator consists of two superconducting Rossendorf type modules, while the injector MAMBO (MilliAMpere BOoster) relies on normal conducting technology. The high power RF system is relying completely on solid-state technology. After some in-depth testing of a 15 kW prototype amplifier in 2017-2019 a modified version of the amplifier module was developed.

In 2020 series production has begun at JEMA France and first amplifiers, a 74 kW, a 56 kW and two 15 kW have been delivered to KPH. In this paper we will present the results of performance testing the amplifiers.

INTRODUCTION

MESA [1] is a few turn recirculating electron linac that can be operated in two modes. The first mode is called external beam (EB) mode where a beam of polarised electrons at $T = 155$ MeV and up to $I_b = 150$ μ A ($Q_b = 0.12$ pC) is lead onto the target of the P2-experiment [2] and dumped afterwards. The second mode is the energy recovery (ER) mode for the MESA gas internal target experiment (MAGIX) [3]. Here a beam of $I_b = 1$ mA ($Q_b = 0.77$ pC) of non polarised electrons is recovered from $T = 105$ MeV to injection energy ($T = 5$ MeV) after interaction with a target. For MESA stage-II the beam current delivered to MAGIX will be increased to 10 mA ($Q_b = 7.7$ pC).

The RF budget for the main linac is determined by beam current and energy gain in EB-mode. Beam loading is 5.6 kW per 9-cell cavity of the modified Rossendorf cryomodules [4-6]. Taking into account microphonic detuning and transmission losses the MESA SSPA (solid-state power amplifiers) were specified to 15 kW.

The MAMBO [7] RF budget is determined by the stage-II ER-mode beam current, the energy gain per RF-tank and the ohmic losses (see Table 1 for RF data of the tanks). The MAMBO 1 tank is a graded- β section and therefore has a rather low shunt impedance and thus high loss power. Together with beam loading and transmission losses the MAMBO SSPA were specified to 74 kW for MAMBO 1 and 56 kW for the others.

Table 1: Shunt impedance R_s , quality factor Q_0 and input coupling κ of the MAMBO RF-tanks (MAMBO 1 from simulation). P_c is loss power w.r.t. nominal field $E_{acc} = 0.65$ MV/m. ΔT is energy gain.

	R_s MΩ	Q_0	κ	P_c kW	ΔT MeV
MAMBO 1	46.7	20500	1.3	40.4	1.15
MAMBO 2	93.5	21745	1.84	18	1.25
MAMBO 3	94.3	21430	1.75	18.3	1.25
MAMBO 4	95.2	21642	1.67	18.4	1.25

AMPLIFIER TOPOLOGY

The power amplifiers are based on the 500 W Wolfspeed 50 V LDMOS RF transistor PTVA127002EV. Four transistors make up a 2 kW RF-module. Each transistor is protected from reflected power by an isolator at the output. Some improvements have been made from the prototype [8]:

- for better cooling transistors are now soldered to a cooling plate instead of using thermal paste. Thus the RF board was redesigned.
- Coaxial splitters/combiners and connecting cables were abandoned in favour of stripline splitters/combiners due to heating.
- For added safety directional couplers are situated at the module outputs with a reflected power interlock.

Several modules are connected by coaxial transitions to a waveguide as power combiner at $\lambda/2$ distance. For increasing power density needed to fit the space requirements at MESA the waveguide combiner was modified. Before, all modules have been operated in phase and their antennas were alternating sides. Now two couplers are facing each other and the modules are driven 180° out of phase. The MAMBO SSPA (3×56 kW, 1×74 kW) comprise of three or four racks, respectively (see Fig. 1), while the MESA SSPA (4×15 kW) are housed in a single rack. MAMBO SSPA have two pre-amplifier stages. A dedicated 1 kW pre-amplifier module is used as first stage. Stage two (intermediate gain stage) comprises two 2 kW standard modules in parallel. MESA SSPA only have the 1 kW pre-amplifier stage.

During prototype testing it showed that a variable drain voltage U_d can optimise efficiency at lower output power considerably [8]. So, all amplifiers are capable of reducing U_d on demand.

AMPLIFIER PERFORMANCE

For the performance tests all amplifiers were operated with a resistive waveguide load and without isolator. The drive signal was generated by a frequency generator whose power

* Work supported by DFG Cluster of Excellence “PRISMA+”



Figure 1: Photograph of the 74 kW (left) and the 56 kW (right) MAMBO SSPA at the electronics area. The middle rack houses two Raspberry Pi based interlock units and a PC as local user interface.

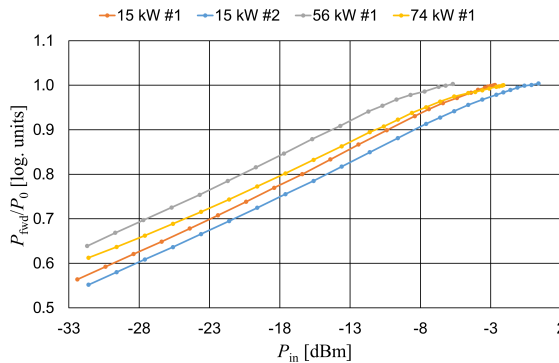


Figure 2: Transmission curves of the amplifiers. Forward power P_{fwd} as function of input power P_{in} . P_{fwd} is normalised to nominal output power P_0 of the respective SSPA at drain voltage $U_d = 50$ V.

P_{gen} was stepped from -30 dBm until the SSPA showed clear signs of compression. P_{gen} was noted and corrected by cable damping to yield input power P_{in} . Forward power P_{fwd} and reflected power were recorded with a power meter from a directional coupler at the waveguide output corrected by the coupling factor. Mostly data at $U_d = 50$ V is presented in the following, but also $U_d = 35$ V, 40 V and 45 V were measured.

P_{fwd} as function of P_{in} (transmission) of all SSPA tested is shown in Fig. 2. It is normalised to the nominal power P_0 of the respective amplifier for easier perception of the diagram. All SSPA reach nominal power.

Gain G was found from the measured data as $G = P_{\text{fwd}} - P_{\text{in}}$ and plotted in Fig. 3. Specification demanded gain flatness of ± 1 dB with power, which is met by all SSPA. 15 kW SSPA #1 provides ca. 2 dB more gain than #2, but this is to some extend due to a difference in cooling water inlet temperature of $\Delta T \approx 4$ °C between both measurements. This differences was caused by weather conditions.

Compression was also determined. This is the deviation of a real amplifier from ideal linear behaviour. Linear amplification is approximated by fitting a straight to the

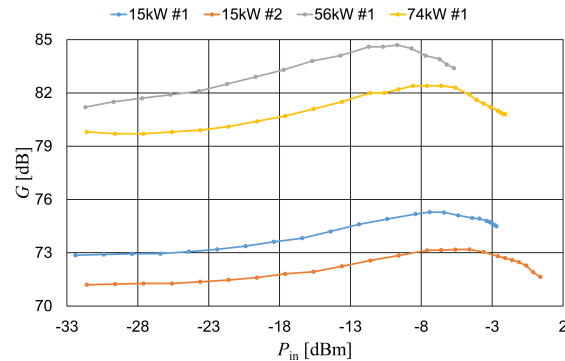


Figure 3: Gain curves at $U_d = 50$ V of the SSPA as function of P_{in} .

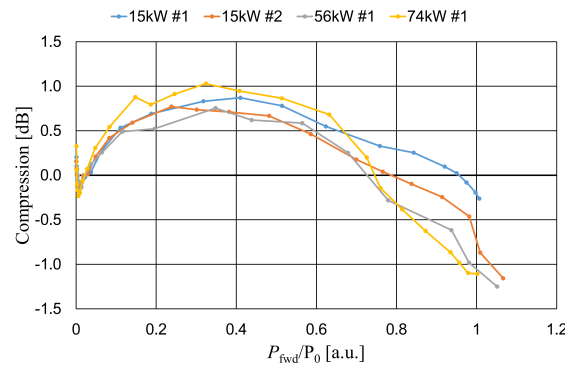


Figure 4: Compression curves at $U_d = 50$ V of all SSPA as function of P_{fwd} . P_{fwd} is normalized to nominal power P_0 of the respective amplifier.

low power signal. Here, using data corresponding to P_{gen} from -30 dBm to -14 dBm (MESA SSPA) and -30 dBm to -18 dBm (MAMBO SSPA), respectively. Different intervals need to be used because of the intermediate gain stage of the MAMBO SSPA. Compression of all SSPA as function of P_{fwd} is compiled into Fig. 4. It was calculated as difference between P_{fwd} and the fitted straight. Abscissa of Fig. 4 is normalised to P_0 of the respective amplifier.

An important figure of merit is the 1 dB-compression point ($P_{1\text{dB}}$), where the real output is 1 dB less than the ideal amplifier. $P_{1\text{dB}}$ can be constructed by either combining P_{fwd} and compression into one diagram as in Fig. 5 and looking up P_{fwd} at P_{in} where compression is -1 dB, or plotting P_{fwd} with the fitted straight into a diagram and shift this straight by -1 dB. So, $P_{1\text{dB}}$ is the intersection point of both graphs in the later case. Both methods yield similar values.

Numerical values of $P_{1\text{dB}}$ gained with method 1 at $U_d = 50$ V are listed in Table 2. For SSPA 15kW#1 $P_{1\text{dB}}$ could not be found since -1 dB compression was not reached before reaching nominal P_{fwd} (see also Fig. 4). Here, SSPA #1 may also have benefited from lower cooling water temperature.

Besides P_{gen} and P_{fwd} also the three AC currents of the 400 V primary power were recorded to get AC power consumption P_{AC} . Wall-plug efficiency η_{AC} was calculated as ratio $\eta_{\text{AC}} = P_{\text{fwd}}/P_{\text{AC}}$. All η_{AC} graphs are quite similar (see

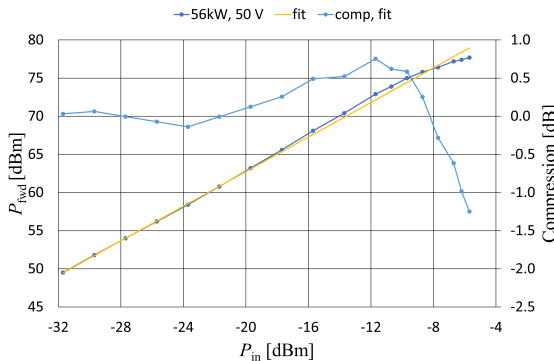


Figure 5: Construction of P1dB of the 56 kW SSPA for example. P_{fwd} and the fitted straight are bound to the left ordinate. Compression as difference of both is bound to the right. P1dB is P_{fwd} at P_{in} where compression is -1 dB .

Table 2: Table of the P1dB compression point of the SSPA at $U_d = 50 \text{ V}$. P1dB of SSPA 15kW#1 exceeds nominal power.

SSPA	P_{in} dBm	P1dB dBm	P1dB kW
15kW #1	n.a.	> 71.79	> 15.1
15kW #2	0.05	71.9	15.49
56kW #1	-6.17	77.415	55.14
74kW #1	-2.37	78.51	70.96

Fig. 6). For P_{fwd} exceeding 90 % nominal power η_{AC} lies between 40 % to 45 %. This can be extended to ca. 45 % nominal power of an amplifier by reducing U_d . Figure 7 shows this for example on the 56 kW SSPA. Efficiency diagrams of the other SSPA look the same. Of course reducing U_d also lowers P1dB.

Bandwidth of the amplifiers was measured at fixed P_{in} for nominal power by varying frequency by $\pm 10 \text{ MHz}$ and recording P_{fwd} . The results are shown in Fig. 8. The decimal resolution measuring the 74 kW SSPA was insufficient,

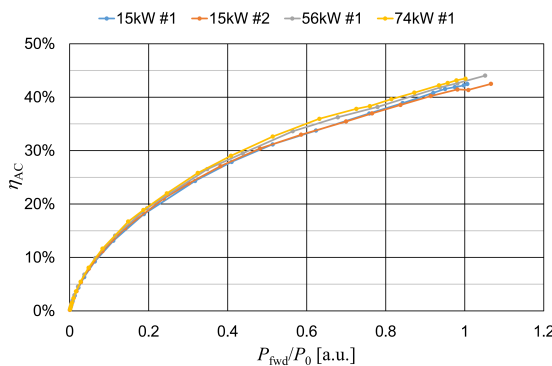


Figure 6: Wall-plug efficiency η_{AC} at $U_d = 50 \text{ V}$ of all SSPA as function of P_{fwd} normalised to their nominal power P_0 in Watt.

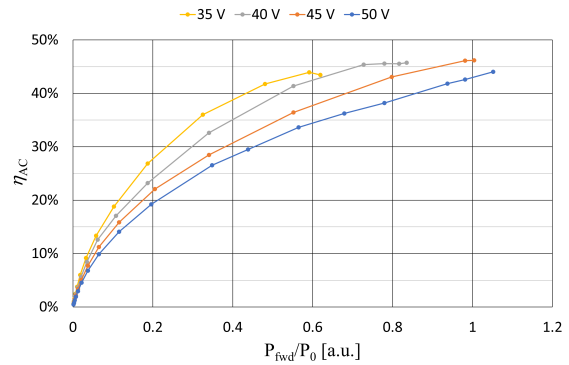


Figure 7: Wall-plug efficiency η_{AC} of the 56 kW SSPA as function of P_{fwd} normalised to $P_0 = 56 \text{ kW}$ at $U_d = 35 \text{ V}$ to 50 V .

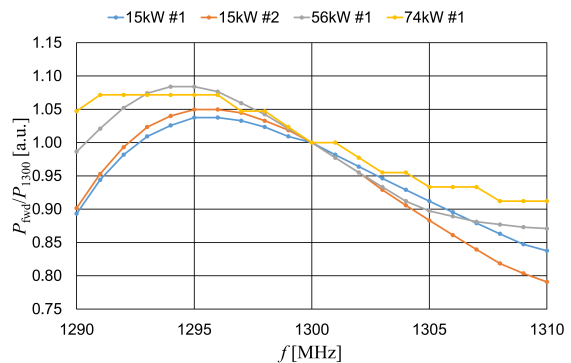


Figure 8: P_{fwd} as function of frequency of the SSPA at fixed P_{in} and $U_d = 50 \text{ V}$, normalised to P_{fwd} at 1.3 GHz (P_{1300}).

therefore the graph is stepped. MESA amplifiers again show some variation.

SUMMARY

All SSPA reach nominal power although the MAMBO 74 kW SSPA does not quite have P1dB as expected. But due to changes in accelerator layout waveguide losses for MAMBO are reduced, so decreased P1dB is not a problem. Comparing both 15 kW amplifiers some spread can be seen. SSPA 15kW#1 performs much better than 15kW#2. It provides roughly 2 dB more gain, shows less compression and a higher bandwidth towards high frequency. Those effects can be explained by the difference in cooling water inlet temperature during experiments. Efficiency is about the same for both.

Delivery of the remaining $2 \times 15 \text{ kW}$ and $4 \times 56 \text{ kW}$ is expected until summer.

REFERENCES

- [1] F. Hug *et al.*, “Status of the MESA ERL-project”, in *Proc. ERL’19*, Berlin, Germany, Sep. 2019, paper MOCOXB05, pp. 14-17. doi:10.18429/JACoW-ERL2019-MOCOXB05
- [2] D. Becker *et al.*, “The P2 experiment”, *Eur. Phys. J. A*, vol. 54, no. 208, (2018). doi:10.1140/epja/i2018-12611-6

- [3] S. Baunack, "Low energy accelerators for high precision measurements", in *Proc. Electromagnetic Interactions with Nucleons and Nuclei Conference (EINN'17)*, Paphos, Cyprus, Oct. 2017, http://einnconference.org/2017/presentations/01_Nov/W2/Baunack.pdf.
- [4] J. Teichert *et al.*, "RF status of superconducting module development suitable for CW operation: ELBE cryostats", *Nucl. Instrum. Meth. Phys. Res., Sect. A*, vol. 557, pp. 239-242, 2006. doi:10.1016/j.nima.2005.10.077
- [5] T. Stengler *et al.*, "Modified ELBE type cryomodules for the Mainz energy-recovering superconducting Accelerator MESA", in *Proc. SRF'15*, Whistler, BC, Canada, Sep. 2015, paper THPB116, pp. 1413-1416, <http://accelconf.web.cern.ch/SRF2015/papers/thpb116.pdf>.
- [6] T. Stengler *et al.*, "Status of the superconducting cryomodules and cryogenic system for the Mainz energy-recovering superconducting accelerator MESA", in *Proc. IPAC'16*, Busan, Korea, May 2016, paper WEPMB009, pp. 2134-2137. doi:10.18429/JACoW-IPAC2016-WEPMB009
- [7] R. Heine, "Preaccelerator concepts for an energy-recovering superconducting accelerator", *Phys. Rev. Accel. Beams*, vol. 24, p. 011602, 2021. doi:10.1103/PhysRevAccelBeams.24.011602
- [8] R. Heine and F. Fichtner, "The MESA 15kW CW 1.3 GHz solid state power amplifier prototype", in *Proc. IPAC'18*, Vancouver, BC, Canada, May 2018, paper THPMF063, p. 4216-4218. doi:10.18429/JACoW-IPAC2018-THPMF063